Luminescent Nitridometal Complexes. Photophysical and Photochemical Properties of the $^3[(d_{xy})^1(d_{\pi^*})^1]$ Excited State of Nitridoosmium(VI) Complexes with Polypyridine Ligands†

Kwok-Fai Chin,[a] Kung-Kai Cheung,[a] Hon-Kay Yip,[a] Thomas C. W. Mak[b] and Chi Ming Che*[,a]

[a] *Department of Chemistry, The University of Hong Kong, Pokfulam Road, Hong Kong*

[b] *Department of Chemistry, The Chinese University of Hong Kong, Shatin, New Territories, Hong Kong*

Nitridoosmium(VI) complexes of substituted 2,2′-bipyridines and 1,10-phenanthrolines have been prepared from $[OsNCl_4]^-$ and the appropriate chelating ligands in acetonitrile. Reaction of $[Os(bipy)NCl_3]$ (bipy = 2,2′-bipyridine) and $[Os(terpy)NCl_2]Cl$ (terpy = 2,2′ : 6′,2″-terpyridine) with neat trifluoromethanesulfonic acid gave $[Os(bipy)NCl_2(H_2O)]^+$ and $[Os(terpy)N(Cl)(CF_3SO_3)]^+$ respectively. The crystal structures of $[Os(dmbipy)NCl_3]$ (dmbipy = 5,5′-dimethyl-2,2′-bipyridine), $[Os(bipy)NCl_2(H_2O)]^+$ and $[Os(terpy)N(Cl)(CF_3SO_3)]^+$ show that the Os≡N distances are 1.68(1), 1.630(7) and 1.629(8) Å respectively. In the latter two complexes the Os≡N moiety is perpendicular to the plane of the chelating ligand. The spectroscopic, photophysical and photochemical properties of the newly prepared complexes have been studied. All have long-lived and emissive $^3[d_{xy},d_{\pi^*}]$ excited states in the solid state and in fluid solution at room temperature. The complex *mer*-$[Os(terpy)NCl_2][ClO_4]$ has the longest emission lifetime 4.64 μs (at infinite dilution) in degassed acetonitrile at room temperature. Based on quenching studies with aromatic hydrocarbons, this complex is a powerful photooxidant with $E^\circ[Os^{VI*}–Os^V]$ being 2.12(30)V *vs.* the normal hydrogen electrode.

Over the past several years the search for luminescent metal complexes for photoinduced atom-transfer reactions has been the subject of our photochemical works.[1–3] We and Gray and co-workers[2–4] demonstrated that d^2 dioxometal complexes such as that of Os^{VI} (refs. 2 and 3) and Re^V (ref. 4) usually have high energy and emissive $^3[(d_{xy})^1(d_{xz},d_{yz})^1]$ states in fluid solutions at room temperature. Interesting photochemistry has been found for *trans*-dioxo(1,4,8,11-tetramethyl-1,4,8,11-tetraazacyclotetradecane)osmium(VI),[2d,5] which is a powerful photooxidant with $E^\circ(Os^{VI*}–Os^V)$ of 2.23 V *vs.* normal hydrogen electrode (NHE) and a lifetime of about 1 μs.

Our research on the photochemistry of d^2 metal complexes has been extended to the nitridoosmium(VI) system.[3] As with *trans*-dioxoosmium(VI), the complexes also have high energy and emissive $^3[(d_{xy})^1(d_{xz},d_{yz})^1]$ excited states in fluid solution. Intriguing photochemistry was found for $[Os(NH_3)_4N]^{3+}$, which undergoes a photoinduced nitrido-coupling reaction leading to the formation of the mixed-valence complex $[Os_2(NH_3)_8(MeCN)_2(\mu\text{-}N_2)]^{5+}$.[3c,e] Of all the nitridoosmium(VI) complexes studied, only $[Os(NH_3)_4N]^{3+}$ has an excited-state lifetime greater than 1 μs. The others have comparably short lifetimes, rendering photochemical studies difficult. As an extension of our study in this area, we aimed to prepare new luminescent nitridoosmium(VI) complexes by treating $[OsNCl_4]^-$ with different chelating ligands. Herein is described the preparation, photophysical and photochemical properties of some complexes of substituted bipyridines, 1,10-phenanthroline and 2,2′:6′,2″-terpyridine (terpy). The crystal structures of $[Os(dmbipy)NCl_3]$ (dmbipy = 5,5′-dimethyl-2,2′-bipyridine), $[Os(terpy)N(Cl)(CF_3SO_3)][CF_3SO_3]$ and $[Os(bipy)NCl_2(H_2O)][CF_3SO_3]$ are also reported.

† *Supplementary data available:* see Instructions for Authors, *J. Chem. Soc., Dalton Trans.*, 1995, Issue 1, pp. xxv–xxx.

Experimental

Materials.—5-Chloro-1,10-phenanthroline (cphen), 4,7-diphenyl-1,10-phenanthroline (dpphen) and 2,2′:6′,2″-terpyridine were obtained from Aldrich. 5,5′-Dimethyl-2,2′-bipyridine[6] and $[NBu_4][OsNCl_4]$[7] were synthesized by literature methods. Trifluoromethanesulfonic acid (CF_3SO_3H) was obtained from Aldrich. All organic chemicals (Aldrich, A.R. grade) for quenching studies were purified by repeated recrystallization or distillation. Acetonitrile (Ajax AR) was distilled over CaH_2. Dichloromethane (Ajax AR) was purified by washing with concentrated H_2SO_4 followed by 5% aqueous Na_2CO_3 and distilled over CaH_2.

Measurements.—The UV/VIS absorption spectra were measured on a Perkin-Elmer Lamda 19 UV/VIS/NIR spectrophotometer, infrared spectra as Nujol mulls on a Nicolet 20-FXC FT-IR spectrophotometer and electronic emission spectra on a Spex Fluorolog-2 spectrofluorometer. Luminescence lifetime and flash-photolysis measurements were performed with a DCR-3 pulsed Nd-YAG laser system.[2d] Sample solutions were degassed by at least four successive freeze–pump–thaw cycles. The absolute emission quantum yield was measured by the method of Demas and Crosby[8] using quinine sulfate in 0.05 mol dm^{-3} sulfuric acid as standard.

Syntheses.—$[Os(dmbipy)NCl_3]$ **1**. The complex was prepared by adding dmbipy (0.2 g) to an acetonitrile solution of $[NBu_4][OsNCl_4]$ (0.5 g in 20 cm^3). The mixture was stirred at about 60 °C for 30 min. A dark purple crystalline solid was obtained after the solution had cooled to room temperature. It was recrystallized by diffusing diethyl ether into an acetonitrile solution. The following complexes were prepared similarly: $[Os(cphen)NCl_3]$ **2** (Found: C, 27.2; H, 1.05; Cl, 25.45; N, 7.90. Calc. for $C_{12}H_7Cl_4N_3Os$: C, 27.40; H, 1.35; Cl, 27.05; N, 8.00%);

[Os(dphen)NCl_3] **3** (Found: C, 44.6; H, 2.70; Cl, 16.40; N, 6.35. Calc. for $C_{24}H_{16}Cl_3N_3Os$: C, 44.8; H, 2.50; Cl, 16.55; N, 6.55%).

mer-[Os(terpy)NX_2][ClO_4] (X = Cl **4** *or* Br **5**)]. An excess of terpy (0.2 g) was added to an acetonitrile solution of [NBu_4][$OsNX_4$] (0.2 g in 20 cm^3) which was stirred for 0.5 h at room temperature. The *mer*-[Os(terpy)NX_2]X complexes were gradually deposited in variable yield (60–80%). The perchlorate salt was obtained by metathesis of the chloride salt with $LiClO_4$ in methanol (Found: C, 29.4; H, 2.0; Cl, 17.4; N, 9.1. Calc.: C, 29.6; H, 1.8; Cl, 17.5; N, 9.2%).

[Os(terpy)N(Cl)(CF_3SO_3)][CF_3SO_3] **6**. Neat trifluoromethanesulfonic acid (2 cm^3) was added to *mer*-[Os(terpy)NCl_2]Cl (0.2 g) in a conical flask. The resulting solution was stirred for about 0.5 h. Yellow solid [Os(terpy)N(Cl)(CF_3SO_3)][CF_3SO_3] was obtained by precipitation with anhydrous diethyl ether. It was recrystallized by diffusing diethyl ether into an acetonitrile solution.

[Os(bipy)NCl_2(H_2O)][CF_3SO_3] **7**. The complex was prepared from [Os(bipy)NCl_3] by a similar procedure to that for **6**. A yellowish brown solid was obtained on addition of anhydrous diethyl ether. The structure was established by an X-ray diffraction analysis.

X-Ray Crystallography.—Crystal data. [Os(dmbipy)NCl_3]·CH_2Cl_2 **1**, M_r = 579.75, triclinic, space group $P\bar{1}$ (no. 2), a = 7.864(3), b = 8.984(2), c = 13.646(3) Å, α = 103.78(2), β = 97.62(2), γ = 92.68(2)°, U = 925.0(4) Å^3, Z = 2, D_c = 2.081 g cm^{-3}, μ(Mo-Kα) = 76.26 cm^{-1}, F(000) = 548. Crystal dimensions 0.06 × 0.10 × 0.22 mm. [Os(terpy)N(Cl)(CF_3SO_3)][CF_3SO_3] **6**, M_r = 771.07, monoclinic, space group $C2/c$, a = 27.568(4), b = 7.863(2), c = 23.552(3) Å, β = 115.54(1)°, U = 4606.4(1.0) Å^3, Z = 8, D_c = 2.224 g cm^{-3}, μ(Mo-Kα) = 59.2 cm^{-1}, F(000) = 2944. Crystal dimensions 0.1 × 0.15 × 0.15 mm. [Os(bipy)NCl_2(H_2O)][CF_3SO_3] **7**, M_r = 598.39, monoclinic, space group $P2_1/n$, a = 10.658(1), b = 9.163(2), c = 17.909(2) Å, β = 92.92(1)°, U = 1746.7(1.0) Å^3, Z = 4, D_c = 2.275 g cm^{-3}, μ(Mo-Kα) = 77.84 cm^{-1}, F(000) = 1128. Crystal dimensions 0.2 × 0.2 × 0.25 mm.

X-Ray diffraction data for complex **1**·CH_2Cl_2 were collected at 294 K on a Nicolet R3m/V four-circle diffractometer using the ω–2θ scan mode with $2\theta_{max}$ = 50° at the Chinese University of Hong Kong. The structure was solved by the Patterson method and refined by least squares. The last least-squares cycle was calculated with 200 parameters (p) and 2642 (n) reflections having $|F_o| > 6\sigma(|F_o|)$ out of 3286 unique reflections, giving R ($= \Sigma||F_o| - |F_c||/\Sigma|F_o|$) = 0.051, R' $\{= [\Sigma w(|F_o| - |F_c|)^2/\Sigma w|F_o|^2]^{\frac{1}{2}}\}$ = 0.065 and S $\{= [\Sigma w(|F_o| - |F_c|)^2/(n-p)]^{\frac{1}{2}}\}$ = 1.845. The weighting scheme was $w = [\sigma^2(F_o) + 0.0005|F_o|^2]^{-1}$. The final Fourier-difference map showed residual extrema in the range 3.07 to −2.12 e Å^{-3}.

Data for complexes **6** and **7** were collected on an Enraf-Nonius CAD-4 diffractometer using the ω–2θ scan mode with $2\theta_{max}$ = 48° at the University of Hong Kong. Intensity data were corrected for Lorentz and polarization effects and empirical absorption based on the ψ scans of four strong reflections. 3897 (3280) Independent reflections were measured, 2890 (2022) of which having $|F_o| \geqslant 6.0\sigma(|F_o|)$ were used in the structure refinement. The structures were solved by Patterson and Fourier methods and subsequent refinement by full-matrix least squares using the Enraf-Nonius SDP programs[9] on a MicroVAX II computer. Convergence for 334 (232) parameters by least-squares refinement on F with $w = 4F_o^2/\sigma^2(F_o^2)$ was reached at R = 0.039 (0.031), R' = 0.049 (0.049) and S = 1.691 (1.350). Final Fourier-difference maps were featureless, with maximum positive and negative peaks of 1.35 (1.50) and 1.53 (1.68 e Å^{-3}) respectively. Tables 1–3 list the atomic coordinates for the non-hydrogen atoms and Table 4 selected bond distances and angles.

Additional material available from the Cambridge Crystallographic Data Centre comprises H-atom coordinates, thermal parameters and remaining bond lengths and angles.

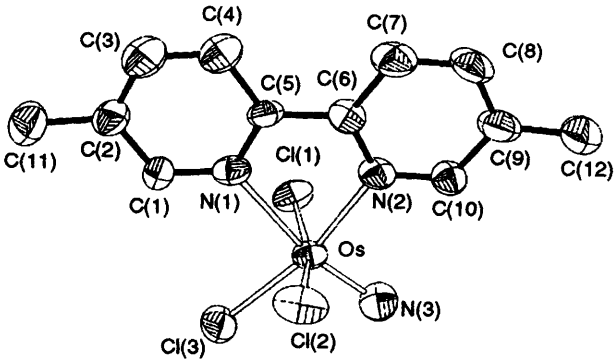

Fig. 1 A perspective view of [Os(dmbipy)NCl_3]

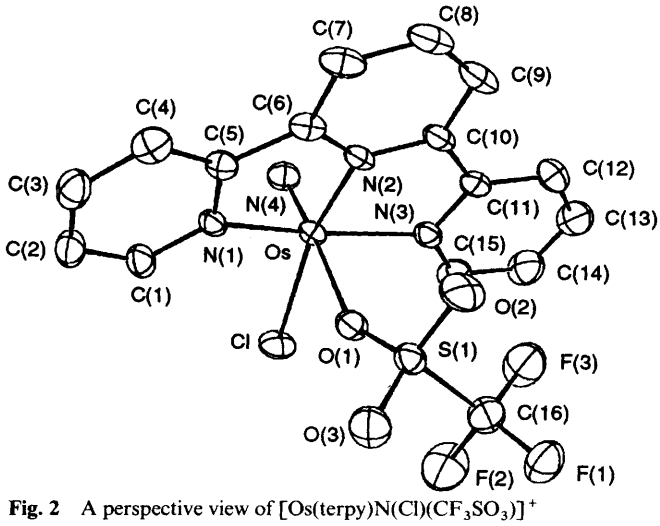

Fig. 2 A perspective view of [Os(terpy)N(Cl)(CF_3SO_3)]$^+$

Results and Discussion

The synthesis of [$OsNCl_3$(L–L)] (L–L = substituted 2,2′-bipyridine or 1,10-phenanthroline) and complex **4** followed the procedures developed by Wright and Griffith.[10] Essentially, treatment of [$OsNCl_4$]$^-$ with the appropriate chelating ligands in acetonitrile gave the desired products, which are air-stable diamagnetic solids. The co-ordinated chloride *trans* to the Os≡N moiety is very substitution labile. Thus, the reaction of **4** and [Os(bipy)NCl_3] with neat CF_3SO_3H gave **6** and **7** respectively in high yields. Meyer and co-workers[11] had previously reported the electrochemical properties and crystal structure of **4**. It is a pale pink solid, stable for a few hours in acetonitrile with exclusion of light. The ν(Os≡N) stretch of **1** and **3** appears at 1084 and 1081 cm^{-1} respectively. Assignment of ν(Os≡N) for **4** and **6** is less clear, as several bands with comparable intensity appear in the range 1050–1100 cm^{-1}. The structures of **1**, **6** and **7** have been established by X-ray diffraction analysis. Perspective views of the molecules are depicted in Figs. 1–3.

Complex **1** adopts a distorted-octahedral co-ordination geometry. The three chlorides are in a *mer* configuration and this is in accordance with the structural assignment for [Os(4,4′-dmbipy)NCl_3] by Ware and Taube.[12] The atoms N(2), Cl(1), Cl(2) and Cl(3) bend away from the nitride ligand with N(2)–Os–Cl(3) angle of 165.4(3)° and Cl(1)–Os–Cl(2) 164.1(1)°. The exceptionally long Os–N(1) distance of 2.32(1) Å reflects the very large *trans* effect of the nitride ligand in this complex. It is indeed longer than the related Os–N (terpy) distance of

2.162(4) Å in $[Os(terpy)NCl_2]Cl$. The Os≡N(3) distance of 1.68(1) Å, however, is slightly longer than the related distance of 1.663(5) Å in $[Os(terpy)NCl_2]Cl$.[11]

As shown in Fig. 2, the structure of complex **7** is quite different from that of **1**. Replacement of one Cl^- by H_2O leads to a change in one of the pyridine moieties of the diimine ligand [equation (1)]. This may be attributed to the weak ligating

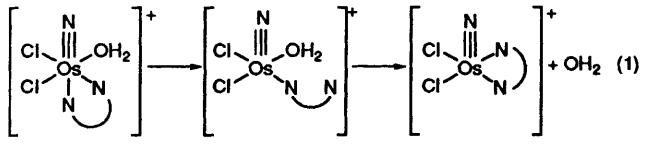

(1)

power of H_2O, which is easily substituted by a pyridyl functional group through an intramolecular process. The Os–Cl distances are comparable to that found in **1**. However, the Os≡N(3) distance of 1.630(7) Å is slightly shorter.

As shown in Fig. 3, the terpy ligand in complex **6** is perpendicular to the Os≡N moiety, quite different from **4** where a coplanar arrangement of the two is found.[11] The Os≡N(4) distance of 1.629(8) Å is shorter than that in **4** and in $[Os(terpy)NCl_2]^+$, but is comparable to that in **7**.

The UV/VIS spectral data for the newly prepared Os^{VI}≡N complexes are listed in Table 5. For illustration, the spectra of **1**, **4** and **6** in acetonitrile are shown in Fig. 4. All these complexes display very intense ($\varepsilon > 10^4$ dm^3 mol^{-1} cm^{-1}) absorption bands at 250–330 nm. Common to all three neutral complexes **1**–**3** is a weak ($\varepsilon < 10^3$ dm^3 mol^{-1} cm^{-1}) and broad absorption ranging from 375 to 511 nm, due to the $d_{xy} \longrightarrow d_{\pi^*}$ transition. A qualitative molecular-orbital diagram for the osmium 5d orbitals of these complexes, according to previous spectroscopic work,[13] is shown in Fig. 5. Not surprisingly, the $d_{xy} \longrightarrow d_{\pi^*}$ transition energy is quite insensitive to the substituents on the aromatic diimine ligands. The UV/VIS spectrum of *mer*-$[Os(terpy)NCl_2]^+$ in acetonitrile deserves some discussion. There is an absorption band centred at about 350 nm, which has large ε_{max} value (8800 dm^3 mol^{-1} cm^{-1}) and shows some vibrational structure. Since a similar absorption band at similar energy has also been found for $[Os(terpy)NBr_2]^+$, this excludes the possibility of it being due to the $P_\pi(X) \rightarrow Os^{VI}$ (X = Cl or Br) charge-transfer transition. It is tentatively assigned to the $P_\pi(N^{3-}) \rightarrow d_{\pi^*}(Os^{VI})$ transition. The average vibrational progression is around 1000 cm^{-1} which is close to the ν(Os≡N)

Table 1 Atomic coordinates of $[Os(dmbipy)NCl_3]\cdot CH_2Cl_2$ **1**

Atom	*x*	*y*	*z*
Os	0.209 63(7)	0.300 17(5)	0.350 44(4)
Cl(1)	−0.083 5(4)	0.314 2(4)	0.367 2(3)
Cl(2)	0.475 8(5)	0.214 6(4)	0.313 8(3)
Cl(3)	0.136 9(5)	0.305 9(4)	0.181 3(3)
N(1)	0.132 5(14)	0.038 0(11)	0.312 8(8)
N(2)	0.260 3(14)	0.234 1(11)	0.489 9(8)
N(3)	0.277 8(16)	0.485 2(12)	0.405 4(9)
C(1)	0.064 4(19)	−0.049 8(14)	0.221 4(9)
C(2)	0.028 3(20)	−0.207 9(14)	0.205 0(11)
C(3)	0.068 9(24)	−0.270 1(15)	0.287 6(12)
C(4)	0.128 4(19)	−0.180 2(14)	0.379 1(11)
C(5)	0.171 0(16)	−0.023 6(13)	0.393 0(9)
C(6)	0.241 7(16)	0.085 0(13)	0.489 7(9)
C(7)	0.290 6(20)	0.038 4(16)	0.578 8(11)
C(8)	0.357 7(23)	0.145 9(16)	0.667 1(10)
C(9)	0.373 1(21)	0.298 2(16)	0.668 0(10)
C(10)	0.326 0(18)	0.336 5(14)	0.576 0(9)
C(11)	−0.046 9(24)	−0.303 3(16)	0.100 4(11)
C(12)	0.447 1(25)	0.418 0(17)	0.760 9(11)
C(13)	0.668 3(25)	0.196 0(20)	0.080 6(13)
Cl(4)	0.605 1(10)	0.311 0(7)	−0.001 6(5)
Cl(5)	0.741 8(8)	0.025 3(6)	0.014 5(5)

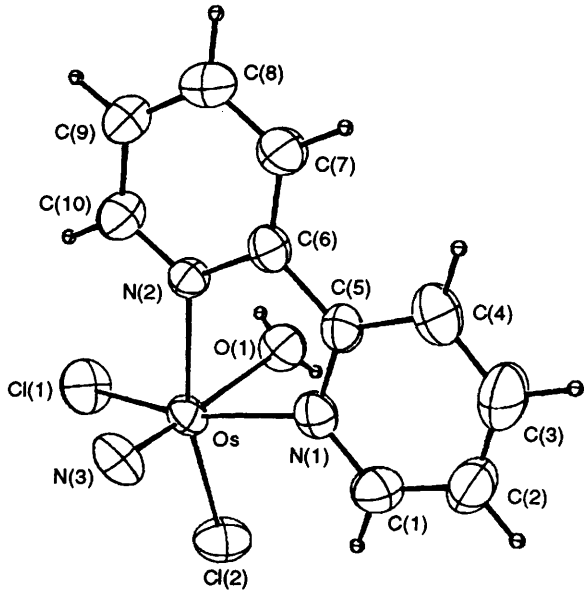

Fig. 3 A perspective view of $[Os(bipy)NCl_2(H_2O)]^+$

Table 2 Atomic coordinates of the non-hydrogen atoms of $[Os(terpy)N(Cl)(CF_3SO_3)][CF_3SO_3]$

Atom	*x*	*y*	*z*	Atom	*x*	*y*	*z*
Os	0.155 16(1)	0.138 92(3)	0.221 63(1)	N(4)	0.182 7(2)	0.203(1)	0.176 6(3)
Cl	0.201 41(8)	−0.118 6(3)	0.255 1(1)	C(1)	0.077 7(3)	−0.110(1)	0.124 5(3)
S(1)	0.090 63(7)	0.057 5(3)	0.325 91(8)	C(2)	0.028 3(4)	−0.159(1)	0.077 7(4)
S(2)	0.394 7(1)	0.957 1(5)	0.458 4(1)	C(3)	−0.014 0(3)	−0.046(1)	0.058 5(4)
F(1)	0.132 5(2)	0.044 5(8)	0.448 3(2)	C(4)	−0.007 1(3)	0.111(1)	0.085 7(4)
F(2)	0.175 9(3)	−0.095 3(9)	0.408 1(3)	C(5)	0.042 8(3)	0.154 3(9)	0.132 8(3)
F(3)	0.181 6(2)	0.171 9(9)	0.412 4(3)	C(6)	0.053 6(3)	0.316(1)	0.167 4(3)
F(4)	0.372 4(5)	0.871(1)	0.548 8(4)	C(7)	0.018 5(3)	0.450(1)	0.160 8(4)
F(5)	0.335 7(4)	1.089(1)	0.505 8(4)	C(8)	0.036 7(3)	0.584(1)	0.201 5(4)
F(6)	0.304 0(4)	0.885(2)	0.455 8(7)	C(9)	0.088 1(3)	0.593(1)	0.248 5(4)
O(1)	0.115 9(2)	0.037 0(7)	0.282 9(2)	C(10)	0.121 8(3)	0.457 2(9)	0.254 3(3)
O(2)	0.069 2(2)	0.223 2(8)	0.323 7(3)	C(11)	0.177 3(3)	0.429(1)	0.303 9(3)
O(3)	0.058 2(2)	−0.083 5(9)	0.324 8(3)	C(12)	0.205 1(4)	0.545(1)	0.352 4(4)
O(4)	0.367 1(3)	1.038(1)	0.400 0(3)	C(13)	0.256 7(4)	0.506(1)	0.396 2(4)
O(5)	0.399 5(4)	0.771(1)	0.448 9(4)	C(14)	0.279 0(4)	0.353(1)	0.392 6(5)
O(6)	0.439 5(4)	1.020(2)	0.506 0(5)	C(15)	0.251 2(3)	0.245(1)	0.344 1(4)
N(1)	0.085 0(2)	0.040 6(8)	0.152 3(3)	C(16)	0.147 2(3)	0.048(1)	0.402 7(4)
N(2)	0.104 8(2)	0.328 1(7)	0.213 5(3)	C(17)	0.347 3(6)	0.942(2)	0.490 8(5)
N(3)	0.202 1(2)	0.281 7(8)	0.300 9(3)				

Table 3 Atomic coordinates of the non-hydrogen atoms of $[Os(bipy)NCl_2(H_2O)][CF_3SO_3]$

Atom	*x*	*y*	*z*
Os	0.271 41(2)	0.246 65(3)	0.359 84(1)
Cl(1)	0.327 9(2)	0.005 1(2)	0.378 2(1)
Cl(2)	0.134 5(2)	0.168 2(3)	0.263 6(1)
S	0.779 2(2)	0.062 6(3)	0.394 6(1)
F(1)	0.865 0(5)	−0.069 3(7)	0.279 4(3)
F(2)	0.733 6(7)	0.097 1(8)	0.252 4(4)
F(3)	0.667 9(7)	−0.100 5(8)	0.294 4(4)
O(1)	0.113 1(5)	0.194 2(7)	0.435 9(3)
O(2)	0.660 6(6)	0.113 0(8)	0.413 7(4)
O(3)	0.868 7(6)	0.177 7(9)	0.387 3(4)
O(4)	0.825 8(8)	−0.059(1)	0.435 3(4)
N(1)	0.180 5(5)	0.444 4(7)	0.370 7(3)
N(2)	0.344 3(5)	0.313 1(7)	0.464 4(3)
N(3)	0.388 2(6)	0.305 7(8)	0.312 9(4)
C(1)	0.099 3(7)	0.503(1)	0.320 0(5)
C(2)	0.042 8(7)	0.637(1)	0.331 7(5)
C(3)	0.071 2(9)	0.708(1)	0.397 7(6)
C(4)	0.153 6(9)	0.649(1)	0.450 3(5)
C(5)	0.208 3(7)	0.514 1(8)	0.435 7(4)
C(6)	0.298 2(6)	0.442 3(8)	0.488 8(4)
C(7)	0.337 6(7)	0.497 1(9)	0.557 0(4)
C(8)	0.423 8(7)	0.421(1)	0.601 4(4)
C(9)	0.472 4(7)	0.293 3(9)	0.575 8(5)
C(10)	0.429 6(7)	0.241 2(8)	0.506 6(5)
C(11)	0.760 8(8)	−0.009(1)	0.301 2(6)

Table 4 Selected bond distances (Å) and angles (°)

$[Os(dmbipy)NCl_3]$ **1**			
Os–Cl(1)	2.353(4)	Os–N(2)	2.12(1)
Os–Cl(3)	2.317(4)	Os–N(1)	2.32(1)
Os–Cl(2)	2.339(4)	Os–N(3)	1.68(1)
Cl(1)–Os–Cl(2)	164.1(1)	Cl(1)–Os–Cl(3)	88.1(1)
Cl(2)–Os–Cl(3)	89.2(1)	Cl(1)–Os–N(1)	82.2(3)
Cl(2)–Os–N(1)	82.2(3)	Cl(3)–Os–N(1)	91.7(3)
Cl(1)–Os–N(2)	90.9(3)	Cl(2)–Os–N(2)	87.8(3)
Cl(3)–Os–N(2)	165.4(3)	N(1)–Os–N(2)	73.7(4)
Cl(1)–Os–N(3)	98.4(4)	Cl(2)–Os–N(3)	97.5(4)
Cl(3)–Os–N(3)	101.6(4)	N(1)–Os–N(3)	166.6(5)
N(2)–Os–N(3)	92.9(5)		
$[Os(terpy)N(Cl)(CF_3SO_3)]^+$ **6**			
Os–Cl(1)	2.342(3)	Os–N(2)	1.986(7)
Os–O(1)	2.289(7)	Os–N(3)	2.082(5)
Os–N(1)	2.069(5)	Os–N(4)	1.629(8)
N(1)–Os–N(4)	98.2(3)	Cl(1)–Os–N(4)	98.6(3)
O(1)–Os–N(4)	177.5(3)	N(3)–Os–N(4)	97.6(3)
N(2)–Os–N(4)	98.2(3)		
$[Os(bipy)NCl_3(H_2O)]^+$ **7**			
Os–Cl(1)	2.313(3)	Os–N(2)	2.081(5)
Os–Cl(2)	2.315(2)	Os–N(1)	2.069(6)
Os–O(1)	2.274(5)	Os–N(3)	1.630(7)
Cl(1)–Os–Cl(2)	87.59(8)	N(2)–Os–N(3)	96.2(3)
Cl(1)–Os–O(1)	84.7(2)	N(1)–Os–N(3)	97.6(4)
Cl(1)–Os–N(3)	101.0(3)	Cl(3)–Os–N(3)	101.6(4)
Cl(2)–Os–N(3)	100.9(2)	N(2)–Os–N(3)	96.2(3)

stretch in the $^3[d_{xy},d_{\pi^*}]$ excited state of $[OsNX_4]^-$.[13] Not surprisingly, it is lower than the ground state ν(Os≡N) of 1090 cm^{-1}. The $d_{xy} \longrightarrow d_{\pi^*}$ transition of *mer*-$[Os(terpy)NX_2]^+$ (X = Cl or Br) probably occurs at around 400–600 nm.

Replacement of a co-ordinated Cl^- by either $CF_3SO_3^-$ or H_2O results in a blue shift in the low-energy absorption spectrum of these Os^{VI}≡N complexes. For example, the lowest-energy absorption band shifts from 511 nm for **1** to 440 nm for **7**. Since **7** has a higher electronic charge than does **1**, stronger

Table 5 The UV/VIS spectral data for $[Os(L)NCl_3]$ in fluid solution at 298 ± 2 K

Complex	λ_{max}/nm (ε_{max}/dm^3 mol^{-1} cm^{-1})
$[Os(dmbipy)NCl_3]^a$	511 (220), 329 (13 000), 273 (15 000)
$[Os(cphen)NCl_3]^a$	512 (220), 368 (2100), 352 (2300), 342 (2400), 282 (21 000), 257 (15 000)
$[Os(dpphen)NCl_3]^a$	512 (240), 375 (5100), 364 (6600), 327 (13 000), 296 (33 000)
$[Os(terpy)NCl_2][ClO_4]^b$	510 (130), 368 (sh) (6800), 353 (8800), 336 (8900), 288 (16 000), 237 (27 000)
$[Os(terpy)NBr_2][ClO_4]^b$	515 (130), 365 (sh) (5800), 342 (7700), 294 (11 000)
$[Os(terpy)N(Cl)(CF_3SO_3)][CF_3SO_3]^b$	368 (11 000), 307 (sh) (7900), 278 (sh) (9800)
$[Os(bipy)Cl_2(H_2O)][CF_3SO_3]^b$	440 (330), 323 (11 000), 247 (sh) (8500), 219 (sh) (22 000)

[a] Measured in CH_2Cl_2. [b] Measured in MeCN.

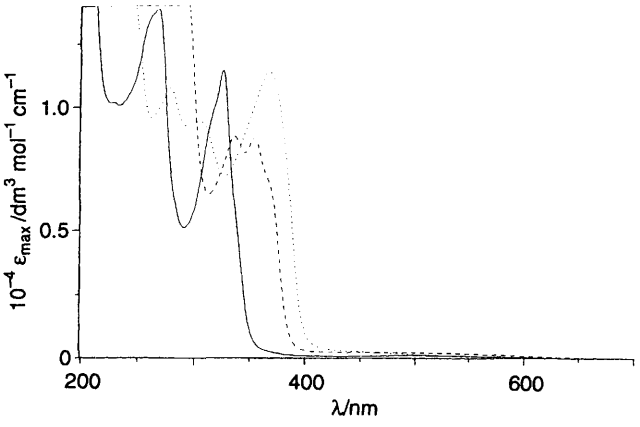

Fig. 4 The UV/VIS absorption spectra of $[Os(dmbipy)NCl_3]$ **1** (—), *mer*-$[Os(terpy)NCl_2][ClO_4]$ **4** (- - -) and $[Os(terpy)N(Cl)(CF_3SO_3)][CF_3SO_3]$ **6** (· · ·) in CH_2Cl_2 (**1**) and MeCN (**4**, **6**) respectively

$P_\pi(N)$–$d_\pi(Os)$ interaction is expected and hence an increase in the $d_{xy} \longrightarrow d_{\pi^*}$ transition energy. This speculation is supported by the X-ray data which reveal a shorter Os≡N distance in **7** than in **1**. Electrochemical data for these complexes measured in MeCN are listed in Table 6. For each of the complexes studied the cyclic voltammogram shows an irreversible reduction wave in the potential range −0.4 to −1.2 V *vs.* 0.1 mol dm^{-3} Ag–$AgNO_3$. For **4**, constant-potential coulometry at −0.7 V established n = 1.0 for this reduction wave. Thus it is due to reduction of Os^{VI} to Os^V. As expected, the E_p value increases with the electronic charge on the metal complexes. Thus, E_p of **6** is 220 mV more anodic than that of **4**.

At room temperature all the complexes show photoluminescence in the solid state and in fluid solution. Fig. 6 shows the emission spectrum of **4** recorded at room temperature and at 77 K. The photophysical data are listed in Table 7. As discussed in previous works, the emission comes from the spin–orbit sublevel of the $^3[(d_{xy})^1,(d_{\pi^*})^1]$ excited state. The substituent on the chelating diimine ligand does not seem to have significant effect on both the emission energy and lifetime of $[Os(L–L)NCl_3]$. However, the emission maximum shifts to higher energy with increase in the electronic charge on the complex. Thus the following order of $\lambda_{max}^{emission}$ is found: **7** < **6** < **4**, **5** < **1**–**3**.

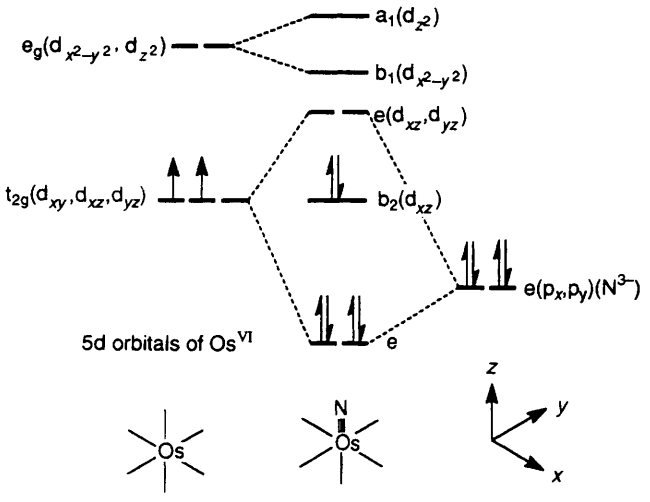

Fig. 5 Simple molecular orbital diagram of a d^2 nitridoosmium complex in C_{4v} symmetry

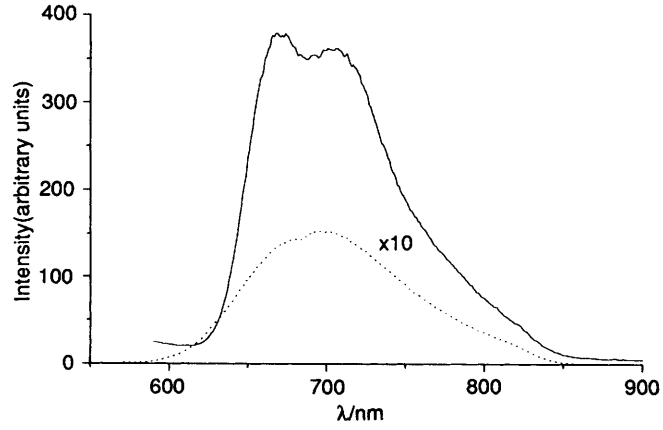

Fig. 6 Emission spectrum of *mer*-[Os(terpy)NCl_2]ClO_2 at room temperature (····) (in degassed acetonitrile) and at 77 K (——) (in *n*-butyronitrile glass)

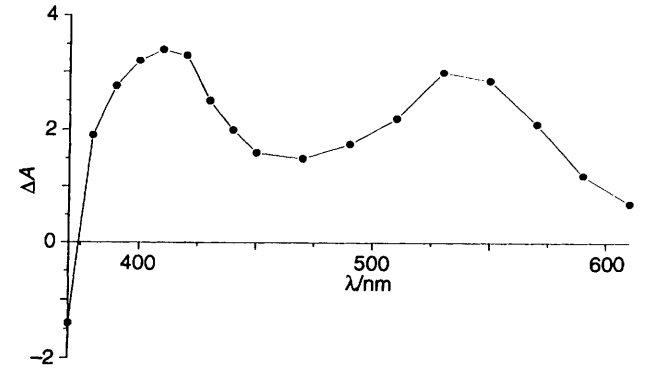

Fig. 7 Transient optical difference absorption spectrum for the $^3[d_{xy},d_{\pi^*}]$ excited state of $[Os(terpy)NCl_2]^+$ (10^{-3} mol dm^{-3}) in acetonitrile. Excitation at 355 nm

Photophysical and Photochemical Properties of Complex **4**.—We chose complex **4** to investigate the excited-state properties since it has a comparatively long emission lifetime of 4.64 μs (at infinite dilution) at room temperature. The absorption spectrum of the $^3[d_{xy},d_{\pi^*}]$ state has been studied. A transient signal with broad absorption at 380–450 and 500–600 nm was recorded 1 μs after flashing (excitation at 355 nm) a degassed acetonitrile solution of the complex (1 mmol dm^{-3}) at room temperature. The transient difference absorption spectrum is shown in Fig. 7. Since the decay rate constant (0.9×10^6 s^{-1}) of this signal matches the phosphorescence lifetime (≈ 1 μs, [Os] = 10^{-3} mol dm^{-3}), the absorption at 380–450 and 500–600 nm arises from the $^3[d_{xy},d_{\pi^*}]$ excited state.

Table 6 Electrochemical data for the nitridoosmium(VI) complexes

Complex	$E^\ominus$ $(Os^{VI}$–$Os^V)^*$/V
[Os(4,4′-dmbipy)NCl_3]	−1.20
[Os(dpphen)NCl_3]	−1.19
[Os(terpy)NCl_2][ClO_4]	−0.62
[Os(terpy)N(Cl)(CF_3SO_3)][CF_3SO_3]	−0.40
[Os(bipy)Cl_2(H_2O)][CF_3SO_3]	−0.78

* The reduction potential was measured in 0.1 mol dm^{-3} [NBu^n_4][PF_6] in MeCN *vs.* Ag–$AgNO_3$.

The excited-state reduction potential was estimated from equation (2) where $E^\ominus$ (Os^{VI*}–Os^V) and $E^\ominus$ (Os^{VI}/Os^V) are the

$$E^\ominus (Os^{VI*}–Os^V) = E_{0-0} + E^\ominus (Os^{VI}–Os^V) \quad (2)$$

redox potentials for the reactions (3) and (4) respectively and

$$Os^{VI*} + e^- \longrightarrow Os^V \quad (3)$$

$$Os^{VI} + e^- \longrightarrow Os^V \quad (4)$$

E_{0-0} refers to the 0–0 emission energy. From the emission spectrum at 77 K the latter is 1.9 eV (*ca.* 3×10^{-19} J). In acetonitrile, complex **4** undergoes an irreversible reduction to Os^V at a potential of −0.62 V *vs.* Ag–$AgNO_3$ (0.1 mol dm^{-3}) (*i.e.* 0.02 V *vs.* NHE). Based on the electrochemical and emission data, $E^\ominus$ (Os^{VI*}–Os^V) is ≥ 1.9 V *vs.* NHE.

As with other Os^{VI}≡N complexes, the $^3[d_{xy},d_{\pi^*}]$ state of **4** undergoes electron-transfer reactions with both inorganic and organic donors. In this work, *mer*-[Os^V(terpy)NCl_2] is generated by a reductive quenching process. Fig. 8 shows the difference absorption spectrum recorded 10 μs after flashing a degassed acetonitrile solution of **4** (≈ 10^{-3} mol dm^{-3}) and $MnCl_2$ (≈ 0.1 mol dm^{-3}). The signal with λ_{max} at 390 nm is stable within 20–50 μs but it gradually decays to a new species having broad absorption at 500–700 nm after 100 ms. This could be due to the formation of a mixed-valence μ-dinitrogen diosmium(II,III) complex, the nature of which awaits further characterization. Since the excited state of *mer*-[Os(terpy)-NCl_2]$^+$ is a powerful oxidant, it is not unreasonable to assign the initial photochemical event to equation (5). A similar

$$mer\text{-}[Os(terpy)NCl_2]^{+*} + Mn^{2+} \longrightarrow Mn^{3+} + mer\text{-}[Os(terpy)NCl_2] \quad (5)$$

transient spectrum was generated with other donors such as $FeCl_2$ and $[Ru(NH_3)_5(MeCN)]^{2+}$.

Previously, we reported the self-quenching behaviour of the emission of $[Os^{VI}(CN)_5N]^{2-}$ and $[Os^{VI}(NH_3)_4N]^{3+}$.[3a,b,e] It is important to know whether similar self-quenching of the emission of complex **4** occurs and thus to ascertain the generality of this photochemical process. The absorption spectrum of **4** obeys Beer's law within a wide range of concentrations (10^{-3}–10^{-4} mol dm^{-3}). This indicates the absence of ground-state interaction among the molecules. From flash photolysis, the emission lifetime has been found to be a function of the complex concentration. A linear Stern–Volmer plot of τ *versus* [Os] was obtained giving the self-quenching rate constant and lifetime at infinite dilution (τ_0) as 7.3×10^8 dm^3 mol^{-1} s^{-1} and 4.64 μs respectively.

The emission of *mer*-[Os(terpy)NCl_2]$^+$ has also been found to be quenched by organic donors (D). Table 8 lists the rate

Table 7 Photophysical data for $[Os(L)NCl_3]$ in degassed dichloromethane and *mer*-$[Os(terpy)NCl_2][ClO_4]$ in acetonitrile at 298 ± 2 K

Complex	Emission (λ_{max}/nm)	$10^8\ k_{self}$/dm^3 mol^{-1} s^{-1}	$\tau_0{}^a$/μs
$[Os(dmbipy)NCl_3]$	730	0.81	0.48
$[Os(cphen)NCl_3]$	732	2.97	0.49
$[Os(dpphen)NCl_3]$	728	0.54	0.57
$[Os(terpy)NCl_2][ClO_4]$	700	7.30	4.64
$[Os(terpy)NBr_2][ClO_4]$	700	6.26	2.33
$[Os(terpy)N(Cl)(CF_3SO_3)][CF_3SO_3]$	660	—	0.20
$[Os(bipy)Cl_2(H_2O)][CF_3SO_3]$	637	—	*b*

[a] Obtained by extrapolating to infinite dilution a plot of τ *vs.* [complex]. [b] Lifetime of the complex varied from sample to sample.

Table 8 Rate constants for quenching of the $^3[d_{xy},d_{\pi^*}]$ excited state of *mer*-$[Os(terpy)NCl_2]^+$ by organic donors in acetonitrile at 298 K

Quencher [$E(D^+-D)$/V *vs.* NHE]	k_q/dm^3 mol^{-1} s^{-1}	ln $k_{q'}$*
N,*N*,*N*′,*N*′-Tetramethyl-*p*-phenylene-diamine [0.34]	1.52×10^{10}	24.9
Triphenylamine [1.02]	1.19×10^{10}	24.1
1,2,4-Trimethoxybenzene [1.36]	8.26×10^{9}	23.4
1,4-Dimethoxybenzene [1.58]	5.76×10^{9}	22.8
1,2,3-Trimethoxybenzene [1.66]	4.05×10^{8}	19.8
1,3,5-Trimethoxybenzene [1.73]	2.56×10^{8}	19.4
Hexamethylbenzene [1.82]	1.05×10^{8}	18.5
Pentamethylbenzene [1.95]	4.94×10^{6}	15.4
1,2,4,5-Tetramethylbenzene [2.03]	2.74×10^{5}	12.5

* $1/k_{q'} = (1/k_q) - (1/k_d)$ where k_d is taken to be 2×10^{10} dm^3 mol^{-1} s^{-1}.

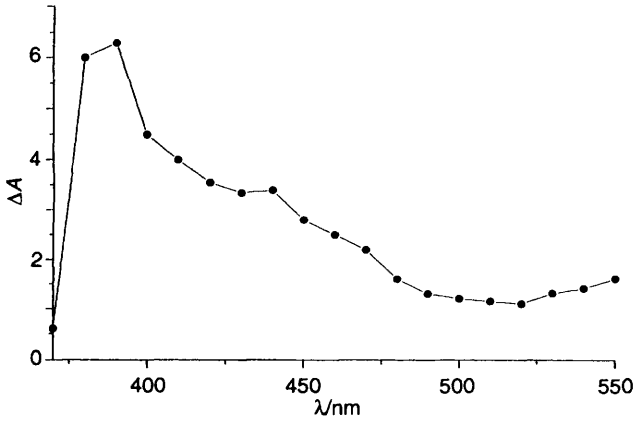

Fig. 8 Transient difference absorption spectrum recorded 10 μs after flash photolysis (at 355 nm) of a degassed acetonitrile solution of *mer*-$[Os(terpy)NCl_2]^+$ (≈ 10^{-3}) and $MnCl_2$ (0.1 mol dm^{-3})

constant k_q and ln $k_{q'}$ ($k_{q'}$ is the rate constant corrected for the diffusion-controlled rate) for quenching by a series of alkylbenzenes. The $k_{q'}$ and the E° (D^+–D) values are fitted *via* a three-parameter, non-linear least-squares analysis of equation (6)[14] where the symbols refers to the reactions (7) and K_{12} =

$$\left(\frac{RT}{F}\right)\ln k_{q'} = \frac{RT}{F}\ln K_{12}\kappa\nu_{23} - \frac{\lambda}{4F}\left(1 + \frac{\Delta G_{23}}{\lambda}\right)^2 \quad (6)$$

$$[Os^{VI}]^{+*} + D \underset{k_{21}}{\overset{k_{12}}{\rightleftharpoons}} [Os^{VI}]^{+*}{\cdot}D \underset{k_{32}}{\overset{k_{23}}{\rightleftharpoons}} Os^{V}{\cdot}D \quad (7)$$

k_{12}/k_{21}, ν_{23} is the effective nuclear vibrational frequency, κ is the electronic transmission coefficient (κ = 1 for a bimolecular

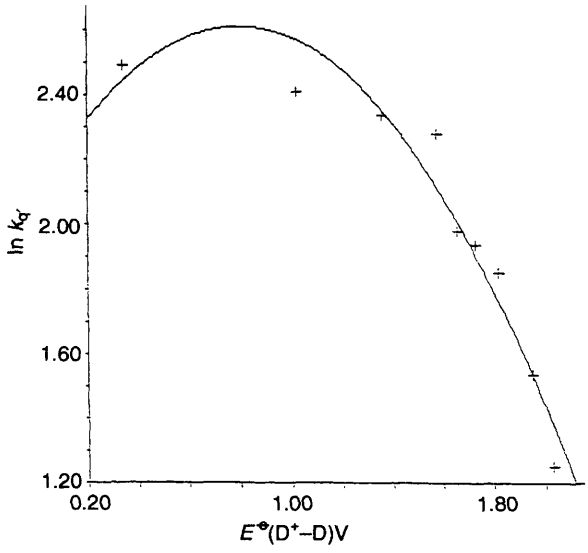

Fig. 9 Plot of ln $k_{q'}$ *versus* $E^\circ(D^+-D)$ for quenching of the $^3[d_{xy},d_{\pi^*}]$ excited state of *mer*-$[Os(terpy)NCl_2]^+$ by aromatic hydrocarbons. (—), Theoretical curve; (+), experimental data

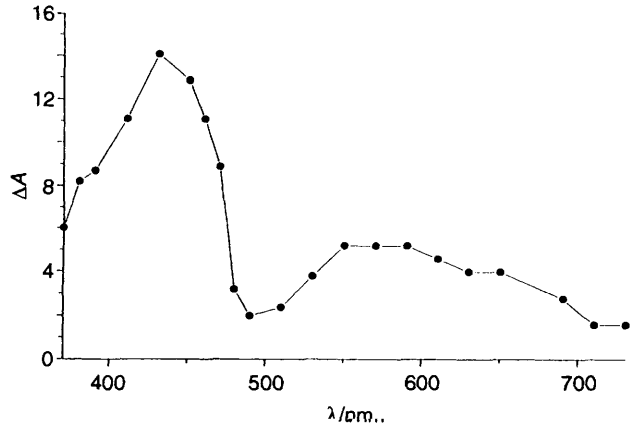

Fig. 10 Transient difference absorption spectrum recorded 5 μs after 355 nm excitation of *mer*-$[Os(terpy)NCl_2]^+$ and *p*-dimethoxybenzene in degassed acetonitrile

electron-transfer reaction), λ is the total reorganization energy associated with the inner and outer co-ordination spheres and ΔG the standard free-energy change of the reaction given by $-[E(Os^{VI*}-Os^{V}) - E(D^+-D)] + w_p - w_r$ where w_r and w_p are work terms for bringing the reactants or products to the mean separation for reaction. For weak interactions, the work terms are due only to coulombic attractions and, therefore, are practically zero when at least one of the two reaction partners is unchanged. Thus, the standard free-energy change of the

electron-transfer step, ΔG(V), can be taken as $-[E(Os^{VI*}-Os^{V}) - E(D^{+}-D)]$.

Fig. 9 depicts both the experimentally determined and theoretically calculated curves. In the region $|\Delta G| \ll 2$ the measured slope of the plot is 0.52, in good agreement with the theoretical value of 0.5 predicted by Marcus theory.[14] From the curve fitting, $E^{\circ}(Os^{VI*}-Os^{V})$, λ and $RT \ln K\kappa\nu$ were 2.12(30) V (*vs.* NHE), 1.32(13) eV and 12.57(10) respectively. The reasonable agreement between experimental data and the prediction by Marcus theory strongly suggests that the quenching process is electron transfer in nature. This is further supported by the observation of long-lived transient signals, λ_{max}(431, 456 nm), due to *p*-dimethoxybenzene radical cation[15] upon the laser flash photolysis of *mer*-$[Os(terpy)NCl_2]^{+}$ and *p*-dimethoxybenzene (10^{-3} mol dm^{-3}) in degassed acetonitrile (Fig. 10). It is noticeable that the value of E° $(Os^{VI*}-Os^{V})$ obtained from data fitting is in line with the lower limit of 1.9 V estimated from the spectroscopic and electrochemical studies described above.

Acknowledgements

We acknowledge support from The University of Hong Kong and the Hong Kong Research Grants Council.

References

1 D. M. Roundhill, H. B. Gray and C. M. Che, *Acc. Chem. Res.*, 1989, **22**, 55; C. M. Che, H. L. Kwong, V. W. W. Yam and K. C. Cho, *J. Chem. Soc., Chem. Commun.*, 1989, 885; C. W. Chan, L. K. Cheng and C. M. Che, *Coord. Chem. Rev.*, 1994, **132**, 87.
2 (*a*) C. M. Che, V. W. W. Yam, K. C. Cho and H. B. Gray, *J. Chem. Soc., Chem. Commun.*, 1987, 948; (*b*) V. W. W. Yam and C. M. Che, *New J. Chem.*, 1989, **13**, 707; (*c*) V. W. W. Yam and C. M. Che, *Coord. Chem. Rev.*, 1990, **97**, 93; (*d*) V. W. W. Yam and C. M. Che, *J. Chem. Soc., Dalton Trans.*, 1990, 3741.
3 (*a*) C. M. Che, T. C. Lau, H. W. Lam and C. K. Poon, *J. Chem. Soc., Chem. Commun.*, 1989, 114; (*b*) C. M. Che, H. W. Lam and T. C. W. Mak, *J. Chem. Soc., Chem. Commun.*, 1989, 1529; (*c*) C. M. Che, H. W. Lam, W. F. Tong, T. F. Lai and T. C. Lau, *J. Chem. Soc., Chem. Commun.*, 1989, 1883; (*d*) H. W. Lam, K. F. Chin, C. M. Che, R. J. Wang and T. C. W. Mak, *Inorg. Chim. Acta*, 1993, **204**, 133; (*e*) H. W. Lam, C. M. Che and K. Y. Wong, *J. Chem. Soc., Dalton Trans.*, 1992, 1411.
4 (*a*) J. R. Winkler and H. B. Gray, *J. Am. Chem. Soc.*, 1983, **105**, 1373; (*b*) J. R. Winkler and H. B. Gray, *Inorg. Chem.*, 1985, **24**, 346.
5 S. Schindler, E. W. Castner, jun., C. Creutz and N. Sutin, *Inorg. Chem.*, 1993, **32**, 4200.
6 G. M. Badger and W. H. F. Sasse, *J. Chem. Soc.*, 1956, 616.
7 W. P. Griffith and D. Pawson, *J. Chem. Soc., Dalton Trans.*, 1973, 1315.
8 J. N. Demas and G. A. Crosby, *J. Phys. Chem.*, 1971, **75**, 346.
9 SDP Structure Determination Package, Enraf-Nonius, Delft, 1985.
10 M. J. Wright and W. P. Griffith, *Transition Met. Chem.*, 1982, **7**, 53.
11 D. W. Pipes, M. Bakir, S. E. Vitols, D. J. Hodgson and T. J. Meyer, *J. Am. Chem. Soc.*, 1990, **112**, 5507.
12 D. C. Ware and H. Taube, *Inorg. Chem.*, 1991, **30**, 4598.
13 C. D. Cowman, W. C. Trogler, K. R. Mann, C. K. Poon and H. B. Gray, *Inorg. Chem.*, 1976, **15**, 1747; M. D. Hopkins, V. M. Miskowski and H. B. Gray, *J. Am. Chem. Soc.*, 1986, **108**, 6908.
14 (*a*) R. A. Marcus, *J. Chem. Phys.*, 1956, **24**, 966; (*b*) C. R. Bock, J. A. Connor, A. R. Gutierrez, T. J. Meyer, D. G. Whitten, B. P. Sullivan and J. K. Nagle, *J. Am. Chem. Soc.*, 1979, **101**, 4815.
15 K. Kawai, N. Yamamoto and H. Tsubomura, *Bull. Chem. Soc. Jpn.*, 1969, **42**, 369.

Received 22*nd August* 1994; *Paper* 4/05110F